



INSTITUT NATIONAL DE RECHERCHE EN INFORMATIQUE ET EN AUTOMATIQUE

*Timestepping schemes for nonsmooth dynamics
based on discontinuous Galerkin methods: definition
and outlook*

Thorsten Schindler, Vincent Acary

N° 7625 — version 2

initial version May 2011 — revised version January 2012

Modeling, Optimization, and Control of Dynamic Systems



*Rapport
de recherche*

Timestepping schemes for nonsmooth dynamics based on discontinuous Galerkin methods: definition and outlook

Thorsten Schindler, Vincent Acary

Theme : Modeling, Optimization, and Control of Dynamic Systems
Équipe-Projet BiPoP

Rapport de recherche n° 7625 — version 2 — initial version May 2011 — revised
version January 2012 — 25 pages

Abstract: The contribution deals with timestepping schemes for nonsmooth dynamical systems. Traditionally, these schemes are locally of integration order one, both in smooth and nonsmooth periods. This is inefficient for applications with infinite events but large smooth phases like circuit breakers, valve trains or slider-crank mechanisms. To improve the behavior during smooth episodes, we start activities twofold. First, we include the classic schemes in time discontinuous Galerkin methods. Second, we split smooth and nonsmooth force propagation. The correct mathematical setting is established with mollifier functions, Clenshaw-Curtis quadrature rules and appropriate impact representation. The result is a Petrov-Galerkin distributional differential inclusion. It defines two Runge-Kutta collocation families and enables higher integration order during smooth transition phases. As the framework contains the classic Moreau-Jean timestepping schemes for constant ansatz and test functions on velocity level, it can be considered as a consistent enhancement. An experimental convergence analysis with the bouncing ball example illustrates the capabilities.

Key-words: timestepping scheme, high order, nonsmooth dynamics, time discontinuous Galerkin methods, experimental convergence analysis, unilateral contact, impact

Schémas à capture d'événements basés sur des méthodes de Galerkin discontinues pour la dynamique non régulière: définition et perspective

Résumé : Ce travail concerne des schémas à capture d'événements pour les systèmes dynamiques non réguliers. Traditionnellement, les méthodes sont d'ordre un dans les périodes régulières et non régulières. Ceci n'est pas efficace pour des applications avec des événements infinis mais avec des périodes régulières grandes comme les disjoncteurs, les distributions ou les liaisons mécaniques. Nous décrivons deux approches pour améliorer le comportement des schémas pendant les épisodes réguliers. D'abord, les schémas classiques sont réformulés dans le cadre des méthodes de Galerkin discontinues. Après, nous décomposons les étapes régulières et non régulières de la propagation de la force. Le cadre mathématique rigoureux est basé sur les fonctions approximatives, le calcul numérique d'une intégrale utilisant Clenshaw-Curtis et une représentation appropriée des impacts. Le résultat est une inclusion différentielle de type Petrov-Galerkin. Elle définit deux familles de méthodes de collocation de type Runge-Kutta et permet l'intégration à l'ordre élevé pendant les transitions régulières. Comme les nouveaux schémas comprennent le schéma classique de Moreau-Jean avec des fonctions d'ansatz et de test constantes pour la vitesse, on peut les voir comme une extension consistante. Une analyse expérimentale de la convergence sur l'exemple de la bille rebondissante montre l'aptitude des méthodes.

Mots-clés : schéma à capture d'événements, ordre élevé, dynamique non régulière, méthode de Galerkin discontinue, analyse expérimentale de la convergence, impact, contact unilatéral

1 Point of Departure

This article discusses higher order timestepping schemes based on time discontinuous Galerkin methods in the context of nonsmooth dynamics. We give a short introduction of nonsmooth dynamical systems, classical time integration schemes and present strategies to achieve higher integration order during smooth episodes.

1.1 Nonsmooth dynamical systems

The *bouncing ball* (cf. Fig. 1) is a typical *nonsmooth dynamical system* in the field of mechanics [20, 27, 13, 6, 21, 19, 2, 23]. Informally, we can envisage the physical evolution

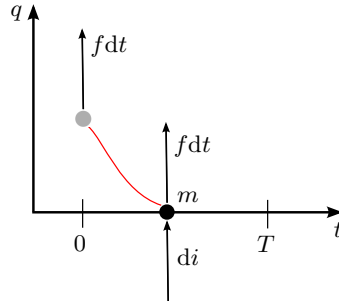


Figure 1: Bouncing ball example.

as follows. During a finite time interval $\emptyset \neq I := (0, T) \subset \mathbb{R}$, a ball with mass m falls from an initial position q_0 , given an initial velocity v_0 and some external *momentum flow* $f dt$. It hits the ground and lifts off again or stays calm depending on the resulting interaction di being partly elastic or plastic. The first case is called a *Zeno phenomenon* if bouncing and free flight alternate infinitely often in I .

The most important realisation is the occurrence of a *velocity jump* due to the *impact*. The function describing the *state* of position and velocity contains smooth and nonsmooth propagation episodes. Using a description based on classical function derivatives, one has to distinguish these two ranges. However, with appropriate mathematical objects, i.e. measures, it is possible to enter the *modern theory* of nonsmooth dynamical systems. Problem 1.1 defines a consistent generalisation of the bouncing ball example, not distinguishing between smooth and nonsmooth motion.

Problem 1.1 (Measure differential inclusion) *Solve the initial value problem*

$$q(0) := q_0 \in \mathbb{R}, \quad (1)$$

$$v(0) := v_0 \in \mathbb{R}, \quad (2)$$

$$dq = v dt, \quad (3)$$

$$dv = m^{-1} f dt + m^{-1} di \quad (4)$$

in terms of measures.

Problem 1.1 is based on the following assumptions.

- dt is the Lebesgue measure of the time t .
- $q \in \mathcal{W}^{1,1}(I)$ is the *absolutely continuous* position with the measure dq .
- $v \in \mathcal{LBV}(I)$ is the velocity of *locally bounded variation* and the weak time derivative of the position q . One can split its measure

$$dv := \gamma dt + \sum_j [[v_j]] \delta_{t_j} := \gamma dt + \sum_j (v_j^+ - v_j^-) \delta_{t_j} \quad (5)$$

in a locally integrable (non-impulsive) and atomic (impulsive) part with

$$\text{accelerations } \gamma \in L^1_{\text{loc}}(I) , \quad (6)$$

$$\text{countable velocity jumps } v_j^\pm \in \mathbb{R} \text{ and Dirac measures } \delta_{t_j} \quad (7)$$

as well as omitting the Cantor part of the singular measure.

- $0 < m^{-1} := m^{-1}(q) \in \mathcal{C}^0(\mathbb{R})$ is the inverse mass.
- $f := f(t, q, v) \in L^1_{\text{loc}}(I \times \mathbb{R} \times \mathbb{R}; \mathbb{R})$ is an external force.
- $i \in \mathcal{LBV}(I)$ is the interaction (impulse) of locally bounded variation. Its measure

$$di := r dt + \sum_j p_j \delta_{t_j} \quad (8)$$

is part of

$$\text{contact relations } (q, v, r, t) \in \mathcal{N}_C , \quad (9)$$

$$\text{countable impact relations } (q_j, v_j, p_j, t_j) \in \mathcal{N}_I \quad (10)$$

and omits the Cantor part of the singular measure. Theoretically, we can write the contact force $r := r(t, q, v) \in L^1_{\text{loc}}(I \times \mathbb{R} \times \mathbb{R}; \mathbb{R})$ as a locally integrable function. In practice, this might not always be obvious. If the contact relation is *single-valued*, the contact force is a (compliant) function of position q , velocity v and time t . However, if the contact relation is *set-valued*, one has to solve nonlinear relations to gain r . The set-valued contact relation may be bilateral, unilateral or may describe a dry friction behaviour.

Interactions may be the root of impulsive behaviour. When a unilateral contact relation closes at time t_j , it has to be evaluated as impact relation to ensure the validity of the constraints after impact time. At this moment, all closed set-valued contact relations are influenced. Hence, also the bilateral and frictional relations have to be considered as impact relations. If one only considered single-valued interactions, then there would not exist any nonsmooth episode of the state variables.

Problem 1.1 is a *measure differential inclusion* (MDI). It uses a weak description of time derivatives in terms of measures. As in the modern theory of partial differential equations (PDE), Problem 1.1 can directly be interpreted in the sense of distributions. We will see that this concept is even more general and that it offers the connection to Galerkin schemes known from the numerical treatment of PDEs. Let $\mathcal{D}(I)$ be the space of all real-valued, C^∞ -functions with compact support and the space of distributions $\mathcal{D}^*(I)$ its dual space. With the primal-dual pairing $\langle *, * \rangle_{\mathcal{D}^*, \mathcal{D}}$ and the distributional derivative $D^1 v$ of v , one achieves the following problem.

Problem 1.2 (Distribution differential inclusion) *Solve*

$$\langle \dot{q}, \varphi_q \rangle_{\mathcal{D}^*, \mathcal{D}} = \langle v, \varphi_q \rangle_{\mathcal{D}^*, \mathcal{D}}, \quad \forall \varphi_q \in \mathcal{D}(I), \quad (11)$$

$$\langle D^1 v, \varphi_v \rangle_{\mathcal{D}^*, \mathcal{D}} = \langle m^{-1} f, \varphi_v \rangle_{\mathcal{D}^*, \mathcal{D}} + \langle m^{-1} di, \varphi_v \rangle_{\mathcal{D}^*, \mathcal{D}}, \quad \forall \varphi_v \in \mathcal{D}(I) \quad (12)$$

together with the initial conditions (1), (2).

Remark 1.3 *Problem 1.2 is characterised by distributions defined by locally integrable functions $L^1_{loc}(I)$ and measures $\mathcal{M}(I)$. These can be identified with subspaces of $\mathcal{D}^*(I)$. Hence, the test functions φ_q and φ_v do not have to be in C^∞ . For the equations to be consistent, condition (12) forces the restrictions. At least function evaluations of φ_v are necessary:*

$$\sum_j [[v_j]] \varphi_v(t_j) = \sum_j m_j^{-1} p_j \varphi_v(t_j). \quad (13)$$

Hence, the test functions for the velocity φ_v must be continuous at the impact times. The position test functions φ_q do not even need to be continuous. However, they should yield finite evaluations of the primal-dual pairings, which is not a problem in practice.

1.2 Integration methods

Timestepping schemes next to event-driven schemes are well-known possibilities to integrate nonsmooth dynamical systems [2].

1.2.1 Classical timestepping schemes

Classical timestepping schemes discretise the equations of motion in Problem 1.1 including the constraints (9), (10) with integration order one. As the time step-size is never adapted in this article, we define a time step-size partition $\mathcal{I} := \{I_1, \dots, I_N\}$ of I initially. The N subintervals $I_i := (t_{i-1}, t_i)$ are of length Δt_i and satisfy

$$0 =: t_0 < t_1 < \dots < t_{N-1} < t_N =: T. \quad (14)$$

This avoids *event* detections, i.e. impact detections: a large number of constraint transitions can be handled with increased computational efficiency when the influence of particular events is not as important as the mean.

Algorithm 1.4 *Classic Moreau-Jean timestepping scheme*

INPUT time interval partition \mathcal{I} , inverse mass m^{-1} , external forces f , impact set \mathcal{N}_I , initial position q_0 , initial velocity v_0 , parameter θ

$i \leftarrow 1$ INITIALIZE LOOP VARIABLE

WHILE $i \leq N$

- solve

$$\left\{ \begin{array}{l} q_i = q_{i-1} + \Delta t_i [(1 - \theta) v_{i-1} + \theta v_i] \\ v_i = v_{i-1} + \Delta t_i [(1 - \theta) m_{i-1}^{-1} f_{i-1} + \theta m_i^{-1} f_i] + m_i^{-1} d_i \\ \text{with } (q_i, v_i, d_i, t_i) \in \mathcal{N}_I \end{array} \right\} \quad (15)$$

- $i \leftarrow i + 1$

Algorithm 1.4 is a representative timestepping scheme. It defines numerical approximations $q_i \approx q(t_i)$, $v_i \approx v(t_i)$, $m_i^{-1} \approx m^{-1}(q_i)$, $f_i \approx f(t_i, q_i, v_i)$, $d_i \approx d_i(t_i, q_i, v_i)$ and does not distinguish between contacts and impacts (cf. Remark 2.4) being evaluated on velocity level. A question of ongoing research is the *solution of the nonlinear expressions* forming the kernel of the algorithm.

1.2.2 Event-driven schemes

Event-driven schemes resolve the exact constraint transition times of Problem 1.1. Between the events, the motion of the system is computed by a classical integration method for *differential algebraic equations* (DAE). This is very accurate but the detection of events can be time consuming and is not possible for Zeno phenomena: the schemes become inconsistent. If an underlying mathematical model exhibits only few events, event-driven schemes are our methods of choice.

1.2.3 Higher order timestepping approaches

We can find two different approaches for achieving consistent higher order timestepping schemes in the literature: augmented timestepping schemes and mixed timestepping schemes.

Augmented timestepping schemes [24, 16] Augmented timestepping schemes are extensions of classical timestepping schemes, e.g. of Moreau-Jean type. If there is no velocity jump during an integration step, one uses classical *augmentation* strategies [11, 14, 15]:

- *Extrapolation* techniques emanating from the basic classical timestepping scheme increase the integration order.
- *Time step-size adaptation* according to Richardson or using embedding methods permit automatic time step-size changes.

Often, the order extrapolation leads to instabilities with closed unilateral constraints because of *chattering* in the classical Aitken-Neville scheme or because of missing *splitting* between smooth and nonsmooth force propagation. Further, order extrapolation cannot conceptually be scheduled in parallel. These items have led to the utilisation of methods with fixed integration order even in the smooth phases. However, the main problem is to find a consistent treatment of nonsmooth episodes. This is usually done by *heuristics*: one uses the classical timestepping scheme and one has to decide about time step-size *adaptation*.

Mixed timestepping schemes [1, 12] Mixed timestepping schemes combine DAE methods for smooth episodes with classical timestepping schemes for nonsmooth phases without resolving the exact constraint transition times. They benefit from the classical theory in smooth segments exactly as augmented timestepping schemes. They are also seriously affected by appropriate time step-size *adaptation* for nonsmooth episodes.

Step-size adaptation Both augmented and mixed procedures suffer mainly from lacking appropriate time step-size adaptation strategies in nonsmooth periods. Usually, one starts from the classical approach based on smooth control theory [11, 14, 15] and uses additional *heuristics* respecting the idea behind timestepping schemes:

- Anticipating gap-estimations [16, 12] or retrospective time step bisection [24], [1, for mixed timestepping] ensure *sufficiently exact detection* of possible velocity jumps.
- *Time step-size switching* $\Delta t_{\text{nonsmooth}} = \mathcal{O}\left(\Delta t_{\text{smooth}}^{p+1}\right)$ couples smooth and nonsmooth regions using the integration order p of the smooth propagation [24], [1, for mixed timestepping].
- Error estimation is based on *not adapted* [16] or *adapted* [1, for classical timestepping] *Richardson strategies* with some additional heuristics, i.e.
 - *exclusion of the possibly jumping velocities* in the error estimation [16], [1, for classical timestepping],
 - discussion of *appropriate norms* [1, for classical timestepping],
 - preferable interval-by-interval *separation* of possible velocity jumps [16, 1],
 - dependence on *penetration* for closed contacts [1, for classical timestepping].

Mainly because of missing smoothness, it is very difficult to derive an appropriate time step-size adaptation respecting the tolerance demands. All mentioned items, i.e. *event prediction*, *norm selection*, *error estimation* and *time step-size selection*, have not been solved satisfactorily for nonsmooth transitions yet. We will have to struggle with exactly the same setting when we prepare timestepping schemes based on time discontinuous Galerkin methods to industrial problems regarding efficiency.

2 Time Discontinuous Galerkin Methods

To consistently improve the behavior during smooth episodes, we embed the classical timestepping schemes in *time discontinuous Galerkin (TDG) methods*. Originally, discontinuous Galerkin (DG) methods have been established for the *space discretisation*. They are special mortar methods and nowadays mainly used for convection-dominated flow problems [5, 9]. If these flow problems exhibit a time-dependence, the time discretisation is canonically given by special Runge-Kutta (RK) schemes. This is fairly not an easy task because of the connection between space and time discretisation due to the Courant-Friedrich-Levy (CFL) condition. Additional stabilisation strategies should e.g. support this crucial relationship. The final Runge-Kutta discontinuous Galerkin methods are of total variation diminishing (TVD), essentially non-oscillatory (ENO) or weighted essentially non-oscillatory (WENO) type [10]. In contrary, we concentrate on the *time discretisation* by DG methods. Our article follows [18], which is considered to be the first contribution. Also [17, 4, 22, 3, 25] have motivated our approach.

DG methods use discontinuous ansatz functions in any situation. In contrast, *extended (XFEM)* or *generalized finite element methods (GFEM)* are based on situation dependant enrichment of a pool of continuous ansatz functions with discontinuous representatives [8]. They are identical developments of two different research groups and follow in general the same ideas as DG methods. We do not consider these methods in the following.

We start from Problem 1.2 and would like to define proper *test functions* and a finite dimensional basis for the discrete solution. We assume:

- test functions might have jumps across the intervals,
- test functions are continuous inside the intervals.

The first assumption leads to the expression of discontinuous Galerkin methods. The second claim states that there is not an instantaneous influence of the analytic nonsmooth dynamics on the numerical solution in-between an interval: the exact time of discontinuity is not resolved. We write $\varphi_q, \varphi_v \in \mathcal{C}^0(\mathcal{I})$ for piecewise-continuous functions with respect to the partition \mathcal{I} .

2.1 Evaluations with discontinuous test functions

It is not clear how to reinterpret (13) if we are using discontinuous test functions and their discontinuities coincide with those of the functional. Depending on the usage of appropriate *mollifiers*, i.e. *smooth cutoff functions*, we define the distributional derivative of a functional $v \in \mathcal{C}^1(\mathcal{I})$ applied to discontinuous functions $\varphi_v \in \mathcal{C}^1(\mathcal{I})$ [3]. Let $\epsilon > 0$ and i an arbitrary index. E.g. with

$$\chi_\epsilon^{i-} : \mathbb{R} \rightarrow \mathbb{R}, \quad t \mapsto \chi_\epsilon^{i-}(t) := \begin{cases} (t - t_{i-1})/\epsilon & \text{for } t_{i-1} \leq t < t_{i-1} + \epsilon \\ 1 & \text{for } t_{i-1} + \epsilon \leq t < t_i \\ 1 + (t_i - t)/\epsilon & \text{for } t_i \leq t < t_i + \epsilon \\ 0 & \text{elsewhere} \end{cases}, \quad (16)$$

we gain an absolutely continuous characteristic mollifier (cf. Fig. 2)

$$\varphi_{v_\epsilon}^{i-} : \mathbb{R} \rightarrow \mathbb{R}, \quad t \mapsto \varphi_{v_\epsilon}^{i-}(t) := \varphi_v(t) \chi_\epsilon^{i-}(t) \quad (17)$$

of φ_v with support in $(t_{i-1}, t_i + \epsilon)$. The integration by parts formula yields

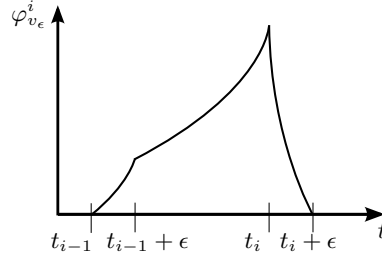


Figure 2: Characteristic mollifier.

$$\begin{aligned} \int D^{1-} v \varphi_{v_\epsilon}^{i-} dt &:= - \int_{t_{i-1}}^{t_{i-1}+\epsilon} v \dot{\varphi}_{v_\epsilon}^{i-} dt - \int_{t_{i-1}+\epsilon}^{t_i} v \dot{\varphi}_{v_\epsilon}^{i-} dt - \int_{t_i}^{t_i+\epsilon} v \dot{\varphi}_{v_\epsilon}^{i-} dt \\ &= [[v_i]] \varphi_{v_\epsilon}^{i-}(t_i) + \int_{t_{i-1}}^{t_i} \dot{v} \varphi_{v_\epsilon}^{i-} dt + \int_{t_i}^{t_i+\epsilon} \dot{v} \varphi_{v_\epsilon}^{i-} dt \end{aligned} \quad (18)$$

because of the continuity of $\varphi_{v_\epsilon}^{i-}$ in $t_{i-1} + \epsilon$ and t_i . In the limit $\epsilon \rightarrow 0$, we use $\chi_\epsilon^{i-}(t_i) = 1$ and the theorem of Lebesgue to achieve

$$\lim_{\epsilon \rightarrow 0} \int D^{1-} v \varphi_{v_\epsilon}^{i-} dt = [[v_i]] \varphi_v(t_i^-) + \int_{t_{i-1}}^{t_i} \dot{v} \varphi_v dt. \quad (19)$$

Hence, we define with a *partition of unity* ansatz

$$\langle D^{1-} v, \varphi_v \rangle_{\mathcal{D}^*, \mathcal{D}} := \sum_i [[v_i]] \varphi_v(t_i^-) + \sum_i \int_{t_{i-1}}^{t_i} \dot{v} \varphi_v dt. \quad (20)$$

This expression focuses on discontinuities at the right border t_i of I_i . Alternatively incorporating the left border t_{i-1} of I_i with a similar mollifier χ_ϵ^{i+} ,

$$\langle D^{1+} v, \varphi_v \rangle_{\mathcal{D}^*, \mathcal{D}} := \sum_i [[v_{i-1}]] \varphi_v(t_{i-1}^+) + \sum_i \int_{t_{i-1}}^{t_i} \dot{v} \varphi_v dt \quad (21)$$

is also a consistent definition. The discontinuity evaluations also could have been totally omitted, which is physically not satisfactory. Further, both the left and the right border of I_i could have been considered. This would result in two term recursions, i.e. *multi-step methods*, because of the three intervals I_{i-1} , I_i and I_{i+1} play a role in.

We use the expression di^\pm instead of di for the interaction measure.

2.2 Timestepping schemes based on time discontinuous Galerkin methods

We demonstrate the numerical approximation of Problem 1.1 with time discontinuous Galerkin methods and discuss its properties.

2.2.1 Definition of the Galerkin approximation

Let $\Phi_q^h, \Phi_v^h \subset \mathcal{C}^0(\mathcal{I})$ be finite dimensional subspaces for test functions with respective bases $\mathcal{B}_{\Phi_q^h} := \{\varphi_{q_k}^h\}_k$ and $\mathcal{B}_{\Phi_v^h} := \{\varphi_{v_k}^h\}_k$. Let further $\Psi_q^h, \Psi_v^h \subset \mathcal{LBV}(I)$ be conforming subspaces for the choice of q - and v -*ansatz functions*. The corresponding bases are given by $\mathcal{B}_{\Psi_q^h} := \{\psi_{q_k}^h\}_k$ and $\mathcal{B}_{\Psi_v^h} := \{\psi_{v_k}^h\}_k$. Then,

$$q^h : I \rightarrow \mathbb{R}, \quad t \mapsto q^h(t) := q_0 + \sum_k \int_{t_0}^t \psi_{q_k}^h ds \dot{q}_k^h, \quad (22)$$

$$v^h : I \rightarrow \mathbb{R}, \quad t \mapsto v^h(t) := \sum_k \psi_{v_k}^h(t) v_k^h \quad (23)$$

is a representation of the numerical solution. The weights $\{\dot{q}_k^h\}_k$ and $\{v_k^h\}_k$ are specified later. Inserting these expressions into Problem 1.2 yields the discrete problem.

Problem 2.1 (Petrov-Galerkin distribution differential inclusion) *Solve*

$$\sum_k \langle \psi_{q_k}^h, \varphi_{q_l}^h \rangle_{\mathcal{D}^*, \mathcal{D}} \dot{q}_k^h = \sum_k \langle \psi_{v_k}^h, \varphi_{q_l}^h \rangle_{\mathcal{D}^*, \mathcal{D}} v_k^h, \quad \forall \varphi_{q_l}^h \in \Phi_q^h, \quad (24)$$

$$\begin{aligned} \sum_k \langle D^{1\pm} \psi_{v_k}^h, \varphi_{v_l}^h \rangle_{\mathcal{D}^*, \mathcal{D}} v_k^h = & \langle m^{-1} f, \varphi_{v_l}^h \rangle_{\mathcal{D}^*, \mathcal{D}} \\ & + \langle m^{-1} di^\pm, \varphi_{v_l}^h \rangle_{\mathcal{D}^*, \mathcal{D}}, \quad \forall \varphi_{v_l}^h \in \Phi_v^h \end{aligned} \quad (25)$$

together with the discrete initial conditions

$$q^h(0) := q_0 \in \mathbb{R}, \quad (26)$$

$$v^h(0) := v_0 \in \mathbb{R}. \quad (27)$$

It is clear that m^{-1} , f , and di^\pm are evaluated using q^h and v^h .

2.2.2 Comparison with the classical Moreau-Jean timestepping scheme

Problem 2.1 is a general description which does not give appropriate time discretisation schemes in all cases. The quality of the schemes is highly depending on the ansatz and test function subspaces. What are primary drivers for their selection?

- Problem 1.1 depends on an initial value and describes a time-evolutionary solution. Also Problem 2.1 should state an *evolution process* not depending on future information at each point in time.

- Experience has shown that for the description of nonsmooth dynamical systems, *one-step methods* are more appropriate than multi-step methods due to the lack of regularities of the right hand side [2].
- For efficient evaluation of the primal-dual pairings, *easy test and ansatz functions* should be used. They have to represent the smoothness of the analytical problem depending on e.g. external forces but also on constraints.

One possibility to achieve these goals is the selection of *piecewise polynomials*. Choosing piecewise constant spaces $\Phi_q^h = \Phi_v^h = \Psi_{\dot{q}}^h = \Psi_v^h := \mathcal{P}^0(\mathcal{I})$, characteristic functions generate canonical bases $\mathcal{B}_{\Phi_q^h} = \mathcal{B}_{\Phi_v^h} = \mathcal{B}_{\Psi_{\dot{q}}^h} = \mathcal{B}_{\Psi_v^h} := \{\chi^i\}_i$. Focusing on the time interval $I_i \in \mathcal{I}$, we gain well-known classical timestepping schemes as a special case of Problem 2.1. We distinguish the alternative evaluations, i.e. $D^{1\pm}$ and di^\pm .

D^{1+} and di^-

Problem 2.2 (Implicit Moreau-Jean timestepping scheme) For $i \in \mathbb{N}$, solve

$$q_i - q_{i-1} = v_i \Delta t_i, \tag{28}$$

$$v_i - v_{i-1} = \int_{t_{i-1}}^{t_i} m^{-1} f dt + \langle m^{-1} di^-, \chi^i \rangle_{\mathcal{D}^*, \mathcal{D}} \tag{29}$$

together with the discrete initial conditions (26), (27).

Again, m^{-1} , f and di^- are evaluated using q^h and v^h . It is noteworthy that there has been some freedom.

- Due to the scheme in Problem 2.1, it is not stated how to select the weights $\{\dot{q}_k^h\}_k$ and $\{v_k^h\}_k$. We have chosen \dot{q}_k^h and v_k^h to coincide with the values of the numerical solution at the right end of the k th interval (cf. Fig. 3 left panel). The constant

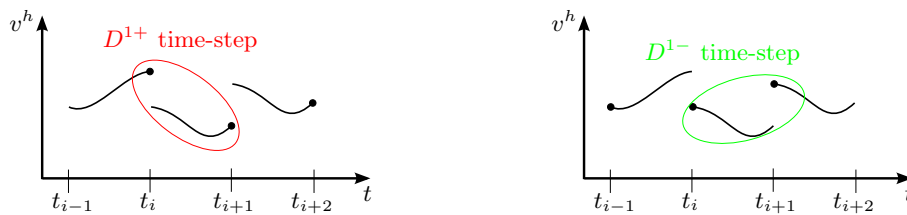


Figure 3: Velocity jump interpretation for D^{1+} and D^{1-} .

velocity in I_i is defined by $v_i = v^h(t_{i+1}^-)$ and the velocity jump, due to D^{1+} , occurs at the *left* side of I_i where the impact, due to di^- , never occurs. The position propagation q_i is derived from \dot{q}_i by the fundamental theorem of calculus.

- The right hand side in (29) is not discretised. We have to choose appropriate quadrature rules which do not depend on discontinuities in the velocity, i.e. select

an appropriate limit $v_l^{h\pm}$ if necessary, and avoid the resolution of impacts:

$$\boxed{\int_{t_{i-1}}^{t_i} m^{-1} f dt \approx (t_i - t_{i-1}) \sum_l \beta_{f_l} m^{-1} (q_l^h) f(t_l, q_l^h, v_l^{h\pm})}, \quad (30)$$

$$\boxed{\langle m^{-1} di^-, \chi^i \rangle_{\mathcal{D}^*, \mathcal{D}} \approx \sum_l m^{-1} (q_l^h) di_l} \quad (31)$$

with $(q_l^h, v_l^h, di_l, t_l) \in \mathcal{N}_I$ on velocity level. The classical Moreau-Jean timestepping scheme ($\theta = 1$) can be achieved with $\beta_{f_1} := 1$, $t_1 := t_i$, $q_1^h = q_i$, $v_1^h = v_i$ and $(q_i, v_i, di_i, t_i) \in \mathcal{N}_I$ on velocity level (cf. Algorithm 1.4).

D^{1-} and di^-

Problem 2.3 (Explicit Moreau-Jean timestepping scheme) For $i \in \mathbb{N}$, solve

$$q_i - q_{i-1} = v_{i-1} \Delta t_i, \quad (32)$$

$$v_i - v_{i-1} = \int_{t_{i-1}}^{t_i} m^{-1} f dt + \langle m^{-1} di^-, \chi^i \rangle_{\mathcal{D}^*, \mathcal{D}} \quad (33)$$

together with the discrete initial conditions (26), (27).

- We have chosen q_k^h and v_k^h to coincide with the values of the numerical solutions at the left end of the k th interval (cf. Fig. 3 right panel). The constant velocity in I_i is defined by $v_{i-1} = v^h(t_i^+)$ and the velocity jump, due to D^{1-} , occurs at the *right* side together with the impact, due to di^- .
- The classical Moreau-Jean timestepping scheme with $\theta = 0$ can be achieved with $\beta_{f_1} := 1$, $t_1 := t_{i-1}$, $q_1^h = q_{i-1}$, $v_1^h = v_{i-1}$ and $(q_i, v_i, di_i, t_i) \in \mathcal{N}_I$ on velocity level (cf. Algorithm 1.4).

D^{1+} / D^{1-} and di^+ With di^+ , all impact evaluations take place in the semi-open interval $[t_{i-1}, t_i)$. The evaluation of the impact laws at the right border of I_i is not maintained by the time discontinuous Galerkin scheme. Repeated tests have shown that this yields poor timestepping schemes [2]. We do not consider this case in the following.

Remark 2.4 Both Problem 2.2 and Problem 2.3 do not distinguish between contacts and impacts. The interaction measure di^- summarises both possibilities and is discretised directly. Hence, there is no splitting

$$\boxed{di_l = (t_i - t_{i-1}) \beta_{r_l} r(q_l^h) + pl} \quad (34)$$

in smooth and nonsmooth interactions and the direct application of higher order schemes would not be successful.

3 Higher Order Timestepping

For the development of higher order timestepping schemes based on time discontinuous Galerkin methods, we start from Problem 2.1. The procedure is similar to the embedding of the Moreau-Jean timestepping scheme in Sect. 2.2.2.

3.1 Selection of bases functions

The following questions arise when defining smooth discrete position and velocity solutions inside an interval I_i . How can integrals with respect to arbitrary functions, e.g. $\langle m^{-1}f, \varphi_{v_l}^h \rangle_{\mathcal{D}^*, \mathcal{D}}$ or $\langle m^{-1}di, \varphi_{v_l}^h \rangle_{\mathcal{D}^*, \mathcal{D}}$, be calculated efficiently? Is it possible to represent also the integrals with respect to polynomials of degree $2M_i$, e.g. $\langle \psi_{q_k}^h, \varphi_{q_l}^h \rangle_{\mathcal{D}^*, \mathcal{D}}$ or $\langle \psi_{v_k}^h, \varphi_{q_l}^h \rangle_{\mathcal{D}^*, \mathcal{D}}$, exactly by the same formula? This demand occurs when discretising I_i with $M_i + 1$ points and nodal ansatz functions. The left and right border of I_i play a special role according to Section 2. How can they be included as integration points? It turns out that the optimal quadrature rules of *Gauß*, *Radau* and *Lobatto* cannot positively respond to all our requirements. Including the borders of I_i as integration points never allows exactness for polynomials of degree $2M_i$. On the other side, *Clenshaw-Curtis* quadrature formulas have positive weights, can be evaluated fast and stable by Fast Fourier Transformation algorithms and are competitive for general integrands as well [26]. We choose the latter methods and mention that it is no drawback that they are exact only for polynomials up to degree M_i . They evaluate the integrand at the *Chebyshev points* $\{t_{i_l}\}_l$ for $M_i \neq 0$. For $M_i = 0$, no rule exists but both $t_{i_0} = t_{i-1}$ and $t_{i_0} = t_i$ are popular choices. The weights with respect to I_i and with respect to its lower subintervals satisfy

$$\beta_{i_l} := \beta_{f_{i_l}} = \beta_{r_{i_l}} = \frac{1}{\Delta t_i} \int_{I_i} l_{i_l} dt, \quad \beta_{i_l}(t^*) := \frac{1}{\Delta t_i} \int_{t_{i-1}}^{t^*} l_{i_l} dt \quad (35)$$

with the classical pruned Lagrange polynomials

$$l_{i_l} : I \rightarrow \mathbb{R}, \quad l_{i_l}(t) := \begin{cases} \prod_{j \neq l} \frac{t - t_{i_j}}{t_{i_l} - t_{i_j}}, & \text{for } t \in I_i \\ 0, & \text{for } t \notin I_i \end{cases}. \quad (36)$$

We use these pruned Lagrange polynomials to define piecewise polynomial nodal bases for test functions $\Phi_q^h = \Phi_v^h := \mathcal{P}^\alpha(\mathcal{I})$ and for ansatz functions $\Psi_q^h = \Psi_v^h := \mathcal{P}^\alpha(\mathcal{I})$. This is a consistent approach, which actually yields a classical Galerkin scheme. Multi-index notation $\alpha := (M_1, \dots, M_N)$ allows for varying polynomial degrees for different elements of \mathcal{I} if needed. Altogether, this results in respective $(N + \sum M_i)$ -dimensional bases $\mathcal{B}_{\Phi_q^h}$, $\mathcal{B}_{\Phi_v^h}$, $\mathcal{B}_{\Psi_q^h}$ and $\mathcal{B}_{\Psi_v^h}$. With $k = \sum_{j=1}^{i-1} (M_j + 1) + l$, their elements satisfy

$$\varphi_{q_k}^h = \varphi_{v_k}^h = \psi_{q_k}^h = \psi_{v_k}^h = l_{i_l}. \quad (37)$$

In the following, we can study easy evaluable one-step evolution processes just by focusing on one interval I_i and by using the related index notation.

3.2 Definition of the general scheme

Stages are the values of position, velocity or acceleration approximations which coincide with the peaks of the nodal bases relative to a sub-interval I_i :

$$q_{i-1,0}^h = q_{i-1}^h, \quad q_{i-1,1}^h = q^h(t_{i_1}), \quad \dots \quad q_{i-1,M_i-1}^h = q^h(t_{i_{M_i-1}}), \quad q_{i-1,M_i}^h = q_i^h, \quad (38)$$

$$\dot{q}_{i-1,0}^h = \dot{q}_{i-1}^{h+}, \quad \dot{q}_{i-1,1}^h = \dot{q}^h(t_{i_1}), \quad \dots \quad \dot{q}_{i-1,M_i-1}^h = \dot{q}^h(t_{i_{M_i-1}}), \quad \dot{q}_{i-1,M_i}^h = \dot{q}_i^{h-}, \quad (39)$$

$$v_{i-1,0}^h = v_{i-1}^{h+}, \quad v_{i-1,1}^h = v^h(t_{i_1}), \quad \dots \quad v_{i-1,M_i-1}^h = v^h(t_{i_{M_i-1}}), \quad v_{i-1,M_i}^h = v_i^{h-}, \quad (40)$$

$$\dot{v}_{i-1,0}^h = \dot{v}_{i-1}^{h+}, \quad \dot{v}_{i-1,1}^h = \dot{v}^h(t_{i_1}), \quad \dots \quad \dot{v}_{i-1,M_i-1}^h = \dot{v}^h(t_{i_{M_i-1}}), \quad \dot{v}_{i-1,M_i}^h = \dot{v}_i^{h-}. \quad (41)$$

We insert the subspace specializations for one interval I_i , i.e. functions like in (37), in Problem 2.1 and we use di^- because of stability reasons (cf. Sect.2.2.2). First, we get the discrete *initial conditions* (26), (27). The position equation of Problem 2.1 yields equations

$$\sum_k \int_{I_i} l_{i_k} l_{i_l} dt \dot{q}_{i-1,k}^h = \sum_k \int_{I_i} l_{i_k} l_{i_l} dt v_{i-1,k}^h \quad (42)$$

for $l \in \{0, \dots, M_i\}$. We have to distinguish if the velocity jump should occur at the left or right interval border (cf. Fig. 3). With (30), (31) and (34), we obtain the following formulations from the velocity equation of Problem 2.1.

3.2.1 Velocity representation: D^{1+}

Search $v_{i-1,M_i}^h = v_i^{h-}$ knowing v_{i-1}^{h-} with equations

$$\begin{aligned} & \left[v_{i-1,0}^h - v_{i-1}^{h-} \right] l_{i_l}(t_{i-1}^+) + \sum_k \int_{I_i} \dot{l}_{i_k} l_{i_l} dt v_{i-1,k}^h = \\ & \Delta t_i \sum_k \beta_{i_k} m_{i_k}^{-1} \left[f_{i_k}^\pm + r_{i_k} \right] l_{i_l}(t_{i_k}^\pm) + \sum_k m_k^{-1} p_k l_{i_l}(t_{i_k}^-), \quad \text{for } l \in \{0, \dots, M_i\}. \end{aligned} \quad (43)$$

3.2.2 Velocity representation: D^{1-}

Search v_i^{h+} knowing $v_{i-1,0}^h = v_{i-1}^{h+}$ with equations

$$\begin{aligned} & \left[v_i^{h+} - v_{i-1,M_i}^h \right] l_{i_l}(t_i^-) + \sum_k \int_{I_i} \dot{l}_{i_k} l_{i_l} dt v_{i-1,k}^h = \\ & \Delta t_i \sum_k \beta_{i_k} m_{i_k}^{-1} \left[f_{i_k}^\pm + r_{i_k} \right] l_{i_l}(t_{i_k}^\pm) + \sum_k m_k^{-1} p_k l_{i_l}(t_{i_k}^-), \quad \text{for } l \in \{0, \dots, M_i\}. \end{aligned} \quad (44)$$

3.2.3 Impact representation

We assume that the discrete velocity behaviour inside an interval is continuously represented by the stage propagation. Hence, impacts are only allowed at the interval borders:

$$\sum_k m_k^{-1} p_k l_{i_l}(t_{i_k}^-) = m_i^{-1} p_i l_{i_l}(t_i^-) \quad (45)$$

with $(q_i^h, v_i^{h\pm}, p_i, t_i) \in \mathcal{N}_I$ on velocity level. For D^{1+} , we use v_i^{h-} , and for D^{1-} , we use v_i^{h+} (cf. Fig. 3). The value p_i equals the right limit of the interaction impulse at t_i .

3.2.4 Weighting integral representation: *reduced* evaluation [18]

The order of the *local error* is governed by the evaluation of (30), (31) and (34) with quadrature rules. Without changing the order, we approximate the weighting integrals in (42), (43) and (44)

$$\sum_k \int_{I_i} l_{i_k} l_{i_l} dt \dot{q}_{i-1,k}^h \stackrel{\text{C-C}}{\approx} \Delta t_i \sum_k \beta_{i_k} \dot{q}_{i-1,k}^h l_{i_l} (t_{i_k}^\pm) = \Delta t_i \beta_{i_l} \dot{q}_{i-1,l}^h, \quad (46)$$

$$\sum_k \int_{I_i} l_{i_k} l_{i_l} dt v_{i-1,k}^h \stackrel{\text{C-C}}{\approx} \Delta t_i \sum_k \beta_{i_k} v_{i-1,k}^h l_{i_l} (t_{i_k}^\pm) = \Delta t_i \beta_{i_l} v_{i-1,l}^h, \quad (47)$$

$$\sum_k \int_{I_i} \dot{l}_{i_k} l_{i_l} dt v_{i-1,k}^h \stackrel{\text{C-C}}{\approx} \Delta t_i \sum_k \beta_{i_k} \dot{v}_{i-1,k}^h l_{i_l} (t_{i_k}^\pm) = \Delta t_i \beta_{i_l} \dot{v}_{i-1,l}^h \quad (48)$$

by the same quadrature rule according to Clenshaw-Curtis (C-C) [26]. Thereby, we evaluate l_{i_l} at the interior limit $t_{i_k}^\pm$ of the sub-interval borders.

3.2.5 Runge-Kutta representation

Substitution of (46) and (47) into (42) yields the *collocation* of $M_i + 1$ velocity stages $\dot{q}_{i-1,l}^h = v_{i-1,l}^h$. We will search *position* stages $\left\{ q_{i-1,l}^h \right\}_l$ knowing $q_{i-1,0}^h$ with the fundamental theorem of calculus (cf. (54), (55), (59), (60)). The velocity expressions (43) and (44) are simplified to respective $M_i + 1$ equations by evaluating the nodal bases and by inserting (48):

$$\left. \begin{array}{l} D^{1+} : \left[v_{i-1,0}^h - v_{i-1}^{h-} \right] l_{i_l} (t_{i-1}^+) \\ D^{1-} : \left[v_i^{h+} - v_{i-1,M_i}^h \right] l_{i_l} (t_i^-) \end{array} \right\} = \Delta t_i \beta_{i_l} \left\{ m_{i_l}^{-1} \left[f_{i_l}^\pm + r_{i_l} \right] - \dot{v}_{i-1,l}^h \right\} + m_i^{-1} p_i l_{i_l} (t_i^-). \quad (49)$$

For *constant ansatz functions* and appropriate definition of the integration point, e.g. either t_i or t_{i-1} , Equation (49) reduces to the implicit or explicit Moreau-Jean timestepping scheme. For *at least linear ansatz functions*, condition (49) expresses velocity jumps

$$D^{1+} : v_{i-1,0}^h = v_{i-1}^{h-} + \Delta t_i \beta_{i_0} \left\{ m_{i_0}^{-1} \left[f_{i_0}^+ + r_{i_0} \right] - \dot{v}_{i-1,0}^h \right\}, \quad (50)$$

$$D^{1-} : v_i^{h+} = v_{i-1,M_i}^h + \Delta t_i \beta_{i_{M_i}} \left\{ m_{i_{M_i}}^{-1} \left[f_{i_{M_i}}^- + r_{i_{M_i}} \right] - \dot{v}_{i-1,M_i}^h \right\} + m_i^{-1} p_i \quad (51)$$

and respective M_i stage relationships for accelerations in Tab. 1. The values $\dot{v}_{i-1,0}^h$ or \dot{v}_{i-1,M_i}^h are needed for the evaluation of (50) or (51) and are still missing. Fortunately, these are values of the acceleration, which is a polynomial of degree $M_i - 1$ in I_i . This

stage	D^{1+}	D^{1-}
$l = 0$	$\dot{v}_{i-1,0}^h = ?$	$\dot{v}_{i-1,0}^h = m_{i_0}^{-1} [f_{i_0}^+ + r_{i_0}]$
$l \in \{1, \dots, M_i - 1\}$	$\dot{v}_{i-1,l}^h = m_{i_l}^{-1} [f_{i_l} + r_{i_l}]$	
$l = M_i$	$\dot{v}_{i-1,M_i}^h = m_{i_{M_i}}^{-1} [f_{i_{M_i}}^- + r_{i_{M_i}}] + \frac{m_{i_{M_i}}^{-1} p_i}{\Delta t_i \beta_{i_{M_i}}}$	$\dot{v}_{i-1,M_i}^h = ?$

Table 1: Stage relationship for accelerations.

polynomial can be uniquely represented by the known M_i nodal values in Tab. 1 as well as by respective and appropriate pruned Lagrangian bases $\{\tilde{l}_{i_k}^\pm\}_k$ [18]:

$$D^{1+} : \dot{v}^h(t) = \sum_{k=1}^{M_i} \tilde{l}_{i_k}^+(t) \dot{v}_{i-1,k}^h, \quad D^{1-} : \dot{v}^h(t) = \sum_{k=0}^{M_i-1} \tilde{l}_{i_k}^-(t) \dot{v}_{i-1,k}^h. \quad (52)$$

Now, we evaluate the acceleration polynomials at t_{i-1} or t_i and get $\dot{v}_{i-1,0}^h$ or \dot{v}_{i-1,M_i}^h . Equation (52) will be also used to derive stage representations of the velocity with the fundamental theorem of calculus (cf. (57), (58), (61)). With

$$\boxed{\tilde{\beta}_{i_l}^\pm := \frac{1}{\Delta t_i} \int_{I_i} \tilde{l}_{i_l}^\pm dt, \quad \tilde{\beta}_{i_l}^\pm(t^*) := \frac{1}{\Delta t_i} \int_{t_{i-1}}^{t^*} \tilde{l}_{i_l}^\pm dt}, \quad (53)$$

we obtain the following Runge-Kutta interpretation of higher order timestepping schemes based on time discontinuous Galerkin methods.

Problem 3.1 (D^{1+} timestepping scheme) Let M_i positive and $l \in \{0, \dots, M_i\}$ for $i \in \mathbb{N}$. Solve simultaneously for the position

$$q_{i-1,l}^h = q_{i-1}^h + \Delta t_i \sum_k \beta_{i_k}(t_{i_l}) v_{i-1,k}^h, \quad (54)$$

$$q_i^h = q_{i-1}^h + \Delta t_i \sum_k \beta_{i_k} v_{i-1,k}^h \quad (55)$$

and for the velocity

$$v_{i-1,0}^h = v_{i-1}^h + \Delta t_i \beta_{i_0} \left\{ m_{i_0}^{-1} [f_{i_0}^+ + r_{i_0}] - \sum_{k=1}^{M_i} \tilde{l}_{i_k}^+(t_{i-1}^+) m_{i_k}^{-1} [f_{i_k}^- + r_{i_k}] \right\} - \tilde{l}_{i_{M_i}}^+(t_{i-1}^+) \frac{\beta_{i_0} m_{i_0}^{-1} p_i}{\beta_{i_{M_i}}}, \quad (56)$$

$$v_{i-1,l}^h = v_{i-1,0}^h + \Delta t_i \sum_{k=1}^{M_i} \tilde{\beta}_{i_k}^+(t_{i_l}) m_{i_k}^{-1} [f_{i_k}^- + r_{i_k}] + \tilde{\beta}_{i_{M_i}}^+(t_{i_l}) \frac{m_{i_0}^{-1} p_i}{\beta_{i_{M_i}}}, \quad (57)$$

$$v_i^h = v_{i-1,0}^h + \Delta t_i \sum_{k=1}^{M_i} \tilde{\beta}_{i_k}^+ m_{i_k}^{-1} [f_{i_k}^- + r_{i_k}] + \tilde{\beta}_{i_{M_i}}^+ \frac{m_{i_0}^{-1} p_i}{\beta_{i_{M_i}}} \quad (58)$$

together with (26), (27) and $(q_{i-1,k}^h, v_{i-1,k}^h, r_{i_k}, t_{i_k}) \in \mathcal{N}_C$ on acceleration level as well as $(q_i^h, v_i^h, p_i, t_i) \in \mathcal{N}_I$ on velocity level.

Problem 3.2 (D^{1-} timestepping scheme) Let M_i positive and $l \in \{0, \dots, M_i\}$ for $i \in \mathbb{N}$. Solve simultaneously for the position

$$q_{i-1,l}^h = q_{i-1}^h + \Delta t_i \sum_k \beta_{i_k}(t_{i_l}) v_{i-1,k}^h, \quad (59)$$

$$q_i^h = q_{i-1}^h + \Delta t_i \sum_k \beta_{i_k} v_{i-1,k}^h, \quad (60)$$

and for the velocity

$$v_{i-1,l}^h = v_{i-1}^{h+} + \Delta t_i \sum_{k=0}^{M_i-1} \tilde{\beta}_{i_k}^-(t_{i_l}) m_{i_k}^{-1} [f_{i_k}^+ + r_{i_k}], \quad (61)$$

$$v_i^{h+} = v_{i-1,M_i}^h + \Delta t_i \beta_{i_{M_i}} \left\{ m_{i_{M_i}}^{-1} [f_{i_{M_i}}^- + r_{i_{M_i}}] - \sum_{k=0}^{M_i-1} \tilde{l}_{i_k}^-(t_i^-) m_{i_k}^{-1} [f_{i_k}^+ + r_{i_k}] \right\} + m_i^{-1} p_i \quad (62)$$

together with (26), (27) and $(q_{i-1,k}^h, v_{i-1,k}^h, r_{i_k}, t_{i_k}) \in \mathcal{N}_C$ on acceleration level as well as $(q_i^h, v_i^{h+}, p_i, t_i) \in \mathcal{N}_I$ on velocity level.

3.3 Trapezoidal rules

For linear velocity discretisations, Problems 3.1 and 3.2 reduce to trapezoidal rules.

Algorithm 3.3 D^{1+} linear timestepping scheme: 'contemplating' trapezoidal rule

INPUT time interval partition \mathcal{I} , inverse mass m^{-1} , external forces f , contact set \mathcal{N}_C , impact set \mathcal{N}_I , initial position q_0 , initial velocity v_0^-

$i \leftarrow 1$ INITIALIZE LOOP VARIABLE

WHILE $i \leq N$

- solve

$$\left\{ \begin{array}{l} q_{i-1,0} = q_{i-1} \\ q_{i-1,1} = q_{i-1} + \frac{\Delta t_i}{2} \{v_{i-1,0} + v_{i-1,1}\} \\ q_i = q_{i-1} + \frac{\Delta t_i}{2} \{v_{i-1,0} + v_{i-1,1}\} \\ v_{i-1,0} = v_{i-1}^- + \frac{\Delta t_i}{2} \{m_{i-1}^{-1} [f_{i-1}^+ + r_{i-1}^+] - m_i^{-1} [f_i^- + r_i^-]\} - m_i^{-1} p_i \\ v_{i-1,1} = v_{i-1}^- + \frac{\Delta t_i}{2} \{m_{i-1}^{-1} [f_{i-1}^+ + r_{i-1}^+] + m_i^{-1} [f_i^- + r_i^-]\} + m_i^{-1} p_i \\ v_i^- = v_{i-1}^- + \frac{\Delta t_i}{2} \{m_{i-1}^{-1} [f_{i-1}^+ + r_{i-1}^+] + m_i^{-1} [f_i^- + r_i^-]\} + m_i^{-1} p_i \\ (q_{i-1,0}, v_{i-1,0}, r_{i-1}^+, t_{i-1}), (q_{i-1,1}, v_{i-1,1}, r_i^-, t_i) \in \mathcal{N}_C, (q_i, v_i^-, p_i, t_i) \in \mathcal{N}_I \end{array} \right\} \quad (63)$$

- $i \leftarrow i + 1$

RR n° 7625

Algorithm 3.3 is the implicit trapezoidal rule with an implicit retrospect for the first stage $v_{i-1,0}$ of the velocity. The method resembles the classical Moreau-Jean timestepping scheme for $\theta = 1/2$, i.e. Algorithm 1.4, and the two stage Lobatto schemes, IIIA for position and IIIC for velocity [7, 14, 15]. Contacts are evaluated on acceleration level leading to a method for ordinary differential equations (ODE-method), impacts are calculated on velocity level.

Algorithm 3.4 D^{1-} linear timestepping scheme: 'forecasting' trapezoidal rule

INPUT time interval partition \mathcal{I} , inverse mass m^{-1} , external forces f , contact set \mathcal{N}_C , impact set \mathcal{N}_I , initial position q_0 , initial velocity v_0^+

$i \leftarrow 1$ INITIALIZE LOOP VARIABLE

WHILE $i \leq N$

• solve

$$\left. \begin{array}{l} q_{i-1,0} = q_{i-1} \\ q_{i-1,1} = q_{i-1} + \frac{\Delta t_i}{2} \{v_{i-1,0} + v_{i-1,1}\} \\ q_i = q_{i-1} + \frac{\Delta t_i}{2} \{v_{i-1,0} + v_{i-1,1}\} \\ v_{i-1,0} = v_{i-1}^+ \\ v_{i-1,1} = v_{i-1}^+ + \Delta t_i m_{i-1}^{-1} [f_{i-1}^+ + r_{i-1}^+] \\ v_i^+ = v_{i-1}^+ + \frac{\Delta t_i}{2} \{m_{i-1}^{-1} [f_{i-1}^+ + r_{i-1}^+] + m_i^{-1} [f_i^- + r_i^-]\} + m_i^{-1} p_i \\ (q_{i-1,0}, v_{i-1,0}, r_{i-1}^+, t_{i-1}), (q_{i-1,1}, v_{i-1,1}, r_i^-, t_i) \in \mathcal{N}_C, (q_i, v_i^+, p_i, t_i) \in \mathcal{N}_I \end{array} \right\} \quad (64)$$

• $i \leftarrow i + 1$

Algorithm 3.4 is the implicit trapezoidal rule with an explicit Euler forecast for the second stage $v_{i-1,1}$ of the velocity. The procedure is similar to the classical Moreau-Jean timestepping scheme for $\theta = 1/2$, i.e. Algorithm 1.4, and to the two stage Lobatto schemes, IIIA for position and III for velocity [7, 14, 15]. Contacts are evaluated on acceleration level leading to an ODE-method, impacts are calculated on velocity level.

4 Experimental Convergence Analysis

D^{1+} and D^{1-} timestepping schemes are *collocating* ODE-methods inside each smooth interval I_i [11]. Hence, the local error for smooth episodes only depends on the adopted quadrature rule.

Theorem 4.1 (Order of local error) *Using Clenshaw-Curtis quadrature rules, the order of the local error for Problems 3.1 and 3.2 satisfies*

$$p = M_i + 1 \quad (65)$$

in sufficiently smooth intervals I_i .

Proof cf. [11, Theorem 6.40] □

This is very good news: whenever we have a smooth propagation of state and (contact) forces, the local error is automatically of higher order, i.e. the numerical approximation is improved for a consistent integration scheme in general. However, we do not know anything about errors due to velocity or interaction jumps. As they are globally propagated, the *global error* will be affected from them. But how? We analyse exemplarily the bouncing ball in three different situations: *free flight* (Problem 4.2), *rest phase* (Problem 4.3) and a *combination of free flight with finite accumulation of impacts* (Problem 4.4) [1]. We will see that our examples support Theorem 4.1 and indicate an order drop due to jumping velocities or interactions.

The bouncing ball defines a *decoupled* example because there is only one interaction possibility. The analytical solution of our settings is never exactly represented by the numerical approximations. Algorithm 1.4 with $\theta = 1$ proposes piecewise linear position, as well as piecewise constant velocity and interaction discretisations. With Algorithm 3.4, we have piecewise quadratic positions, piecewise linear velocities and piecewise quadratic interactions. In a Python¹ implementation, we paid attention to evaluate the local and global error at least as exact as the timestepping discretisations. SciPy's² *barycentric interpolation* for the velocities, as well as *Hermite interpolation* for positions and interactions are exact and efficient *dense output* formulas [15]. SciPy's *Gauss-Konrod quadrature* provides appropriate error formulas in L^1 -norm for position, velocity and interactions.

Problem 4.2 (Bouncing ball : free flight) *Discuss the scalar initial value problem*

$$q(0) := 1, \quad v(0) := 0, \quad (66)$$

$$\dot{q} = v, \quad \dot{v} = -10t^2 \quad (67)$$

in terms of measures.

The *analytical solution* is given by

$$q(t) = 1 - \frac{5}{6}t^4, \quad v(t) = -\frac{10}{3}t^3, \quad i(t) = 0. \quad (68)$$

During *free flight*, the state is of order two for Algorithm 3.4 and of order one for Algorithm 1.4 with $\theta = 1$ (cf. Fig. 4). The interaction is zero and resolved exactly.

Problem 4.3 (Bouncing ball : rest phase) *Discuss the scalar initial value problem*

$$q(0) := 0, \quad v(0) := 0, \quad (69)$$

$$\dot{q} = v, \quad \dot{v} = -10t^2 + r, \quad (70)$$

$$0 \leq q \perp r \geq 0 \quad (71)$$

in terms of measures.

¹<http://www.python.org/>

²<http://www.scipy.org/>

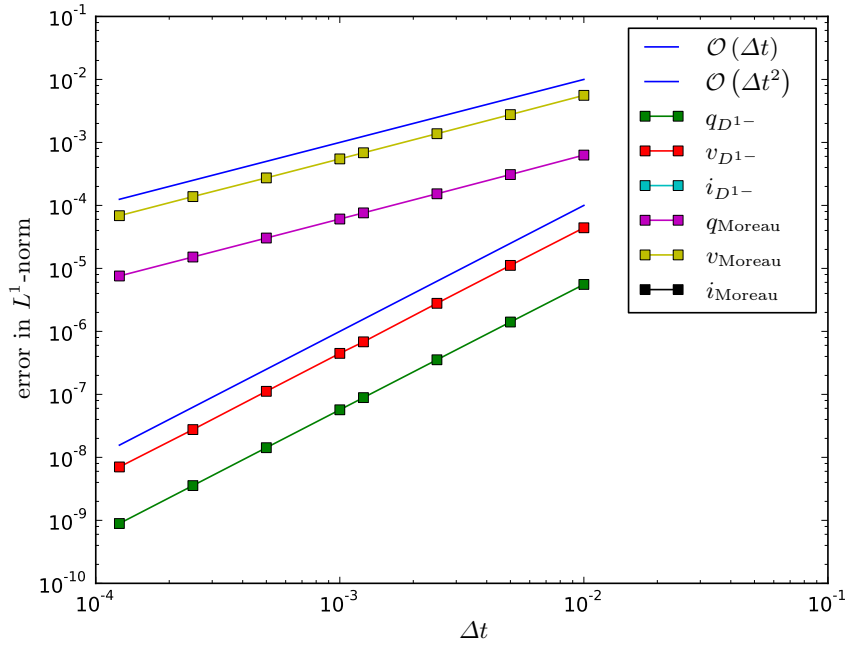


Figure 4: Experimental convergence analysis: free flight.

The *analytical solution* is given by

$$q(t) = 0, \quad v(t) = 0, \quad i(t) = \frac{10}{3} t^3. \quad (72)$$

During *rest phase*, the interaction is of order two for Algorithm 3.4 and of order one for Algorithm 1.4 with $\theta = 1$ (cf. Fig. 5). The state is zero and resolved exactly.

Problem 4.4 (Bouncing ball : combined analysis) *With Newton's restitution coefficient $\epsilon_N = 0.5$, discuss the scalar initial value problem*

$$q(0) := 1, \quad v(0) := 0, \quad (73)$$

$$\dot{q} = v, \quad \dot{v} = -2, \quad (74)$$

$$v_j^+ = v_j^- + \max\{0, -(1 + \epsilon_N) v_j^-\} \text{ if } q_j = 0 \quad (75)$$

in terms of measures.

The *analytical solution* is given by

free flight – $0 \leq t < 1$

$$q(t) = 1 - t^2, \quad v(t) = -2t, \quad i(t) = 0 \quad (76)$$

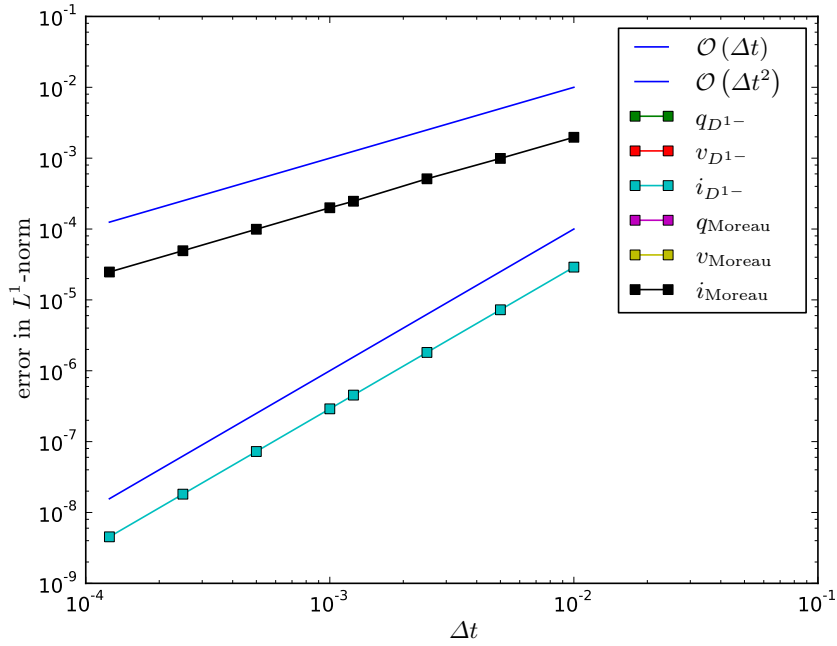


Figure 5: Experimental convergence analysis: rest phase.

$$\text{Zeno state} - \forall n \in \mathbb{N}_0 : 3 - \frac{1}{2^{n-1}} \leq t < 3 - \frac{1}{2^n}$$

$$q(t) = -(t-3)^2 - \frac{3}{2^n}(t-1) + \frac{1}{2^{n-1}} \left(3 - \frac{1}{2^n} \right), \quad (77)$$

$$v(t) = -2(t-3) - \frac{3}{2^n}, \quad (78)$$

$$i(t) = \sum_{k=0}^n \frac{3}{2^k}. \quad (79)$$

For the *combined analysis*, the global error of state and interaction is of order one for both Algorithm 3.4 and Algorithm 1.4 with $\theta = 1$ (cf. Fig. 6).

5 Conclusion

In this paper, we have shortly summarised the state-of-the-art description of nonsmooth dynamical systems with either measure or distribution differential inclusions. Two classic integration methods have been identified for this type of evolution problems: event-driven and timestepping schemes. The intrinsic difficulty of event-driven integration is its high effort of event detection and inconsistency for Zeno phenomena. The drawback of classic timestepping schemes is their low integration order; recently, this had been tackled with

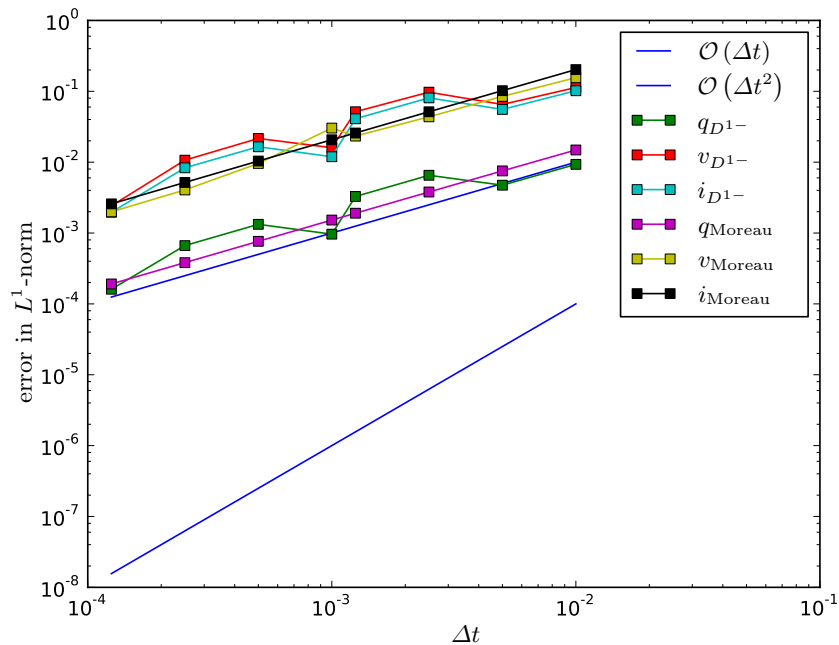


Figure 6: Experimental convergence analysis: combined analysis.

augmentation and mixing. We have proposed a new strategy offering both a consistent embedding in *time discontinuous Galerkin methods*, as well as a *splitting* of smooth and nonsmooth force propagation. The framework has been developed in its full generality with mollifier functions, Clenshaw-Curtis quadrature rules and appropriate impact representation. Altogether, we have stated two Runge-Kutta collocation families as resulting timestepping methods. The order of the local error only depends on the order of the underlying quadrature rule for smooth episodes. Choosing piecewise constant ansatz and test functions on velocity level, the classic explicit and implicit Moreau-Jean timestepping schemes have been found out to be special cases of the general method. For the piecewise linear case, the two families relate to a 'forecasting' and to a 'contemplating' trapezoidal rule. An experimental convergence analysis discusses the bouncing ball example in different episodes. We compare the properties of the constant ansatz to the characteristics of the linear ansatz. Whereas we have always integration order one for the Moreau-Jean timestepping, the new linear scheme offers integration order two in smooth phases. This observation matches exactly the expectations and should be the starting point for further investigations. Can we derive any theoretical results about the global order of timestepping schemes? How can splitting methods improve timestepping schemes, e.g. using general DAE-methods for smooth episodes? What is necessary to define consistent automatic time step-size adaptations for timestepping schemes? Answers

to these questions are important for even more successful time integration of nonsmooth industrial examples.

Acknowledgement

This work has been supported by the French National Research Agency (ANR) through COSINUS program (project SALADYN³ ANR-08-COSI-014). The first author has been granted by an INRIA⁴ postdoctoral fellowship.

References

- [1] ACARY, Vincent: Higher order event capturing time-stepping schemes for nonsmooth multibody systems with unilateral constraints and impacts. In: *Appl Numer Math* (to appear 2011). – ISSN 0168–9274
- [2] ACARY, Vincent ; BROGLIATO, Bernard: *Lecture notes in applied and computational mechanics*. Vol. 35: *Numerical methods for nonsmooth dynamical systems : applications in mechanics and electronics*. 1st edition. Berlin : Springer, 2008. – ISBN 3–540–75391–5
- [3] ALBERTY, Jochen ; CARSTENSEN, Carsten: Discontinuous Galerkin time discretization in elastoplasticity: motivation, numerical algorithms, and applications. In: *Comput Methods Appl Mech Engrg* 191 (2002), Nr. 43, pp. 4949–4968. – ISSN 0045–7825
- [4] BAUCHAU, Olivier: Computational schemes for flexible, nonlinear multi-body systems. In: *Multibody System Dynamics* 2 (1998), Nr. 2, pp. 169–225. – ISSN 1573–272X
- [5] BERNARDI, Christine ; MADAY, Yvon ; PATERA, Anthony: A new nonconforming approach to domain decomposition: The mortar element method. In: BRÉZIS, Haïm (Hrsg.): *Nonlinear partial differential equations and their applications* Vol. 302. Harlow : Longman, 1994. – ISBN 0–582–23801–3, pp. 13–51
- [6] BROGLIATO, Bernard ; DAM, Tonny ten ; PAOLI, Laetitia ; GENOT, Frank ; ABADIE, Michel: Numerical simulation of finite dimensional multibody nonsmooth mechanical systems. In: *Appl Mech Rev* 55 (2002), pp. 107–150. – ISSN 0003–6900
- [7] BUTCHER, John: *Numerical methods for ordinary differential equations*. 2nd edition. Chichester[u.a.] : Wiley, 2008. – ISBN 978–0–470–72335–7
- [8] CHESSA, Jack ; BELYTSCHKO, Ted: Arbitrary discontinuities in space-time finite elements by level sets and XFEM. In: *Int J Numer Meth Eng* 61 (2004), Nr. 15, pp. 2595–2614. – ISSN 0029–5981

³<http://saladyn.inria.gforge.fr/>

⁴<http://www.inria.fr/>

- [9] COCKBURN, Bernardo: Discontinuous Galerkin methods. In: *J Appl Math Mech* 83 (2003), Nr. 11, pp. 731–754. – ISSN 0044–2267
- [10] COCKBURN, Bernardo ; SHU, Chi-Wang: Runge-Kutta Discontinuous Galerkin Methods for Convection-Dominated Problems. In: *J Sci Comput* 16 (2001), Nr. 3, pp. 173–261. – ISSN 0885–7474
- [11] DEUFLHARD, Peter ; BORNEMANN, Folkmar: *Texts in applied mathematics*. Vol. 42: *Scientific computing with ordinary differential equations*. New York : Springer, 2002. – ISBN 0–387–95462–7
- [12] ESEFELD, Bastian ; ULBRICH, Heinz: A Hybrid Integration Scheme For Nonsmooth Mechanical Systems. In: *Multibody Dynamics 2011, Eccomas Thematic Conference, Brussels, 4th until 7th July 2011*, to appear 2011
- [13] GLOCKER, Christoph: *Lecture notes in applied and computational mechanics*. Vol. 1: *Set-valued force laws in rigid body dynamics : dynamics of non-smooth systems*. 1st edition. Berlin : Springer, 2001. – ISBN 978–3–540–41436–0
- [14] HAIRER, Ernst ; WANNER, Gerhard: *Springer series in computational mathematics*. Vol. 8: *Solving Ordinary Differential Equations: Nonstiff Problems*. 2nd rev. edition, 1st softcover printing. Berlin : Springer, 2009. – ISBN 978–3–642–05163–0
- [15] HAIRER, Ernst ; WANNER, Gerhard: *Springer series in computational mathematics*. Vol. 14: *Solving Ordinary Differential Equations II: Stiff and Differential-Algebraic Problems*. 2nd rev. edition, 1st softcover printing. Berlin : Springer, 2010. – ISBN 978–3–642–05220–0
- [16] HUBER, Robert ; ULBRICH, Heinz: Higher Order Integration of Non-Smooth Dynamical Systems Using Parallel Computed Extrapolation Methods Based on Time-Stepping Schemes. In: *Proceedings of 1st Joint International Conference on Multibody System Dynamics, Lappeenranta, 25th-27th May 2010*, 2010. – ISBN 978–952–214–778–3
- [17] JOHNSON, Claes: Error estimates and adaptive time-step control for a class of one-step methods for stiff ordinary differential equations. In: *SIAM J Numer Anal* 25 (1988), Nr. 4, pp. 908–926. – ISSN 0036–1429
- [18] LASAINT, Pierre ; RAVIART, Pierre-Arnaud: On a finite element method for solving the neutron transport equation. In: *Symposium on Mathematical Aspects of Finite Elements in Partial Differential Equations, Madison, 1st until 3rd April 1974*, 1974. – ISBN 0–12–208350–4
- [19] LEINE, Remco I. ; WOUW, Nathan van d.: *Lecture notes in applied and computational mechanics*. Vol. 36: *Stability and convergence of mechanical systems with unilateral constraints*. Berlin : Springer, 2008. – ISBN 978–3–540–76975–0

-
- [20] MOREAU, Jean J.: Bounded variation in time. In: *Topics in Nonsmooth Mechanics*. Basel : Birkhäuser, 1988. – ISBN 3-7643-1907-0, pp. 1-74
- [21] PFEIFFER, Friedrich: *Lecture notes in applied and computational mechanics*. Vol. 40: *Mechanical system dynamics*. corr. 2nd printing. Berlin : Springer, 2008. – ISBN 978-3-540-79435-6
- [22] SCHÖTZAU, Dominik ; SCHWAB, Christoph: Time discretization of parabolic problems by the hp-version of the discontinuous Galerkin finite element method. In: *SIAM J Numer Anal* 38 (2000), Nr. 3, pp. 837-875. – ISSN 0036-1429
- [23] STEWART, David: *Dynamics with inequalities*. Philadelphia : SIAM, 2011. – ISBN 978-1-611-97071-5
- [24] STUDER, Christian: *Lecture notes in applied and computational mechanics*. Vol. 47: *Numerics of unilateral contacts and friction : modeling and numerical time integration in non-smooth dynamics*. Berlin : Springer, 2009. – ISBN 978-3-642-01099-6
- [25] THOMÉE, Vidar: *Galerkin finite element methods for parabolic problems*. 2nd edition. Berlin : Springer, 2006 (Springer series in computational mathematics ; 25). – ISBN 978-3-540-33121-6
- [26] TREFETHEN, Lloyd: Is Gauss Quadrature Better than Clenshaw-Curtis? In: *SIAM Rev* 50 (2008), Nr. 1, pp. 67-87. – ISSN 0036-1445
- [27] TRINKLE, Jeffrey ; PANG, Jong-Shi ; SUDARSKY, Sandra ; LO, Grace: On dynamic multi-rigid-body contact problems with Coulomb friction. In: *J Appl Math Mech* 4 (1997), pp. 267-279. – ISSN 0044-2267



Centre de recherche INRIA Grenoble – Rhône-Alpes
655, avenue de l'Europe - 38334 Montbonnot Saint-Ismier (France)

Centre de recherche INRIA Bordeaux – Sud Ouest : Domaine Universitaire - 351, cours de la Libération - 33405 Talence Cedex
Centre de recherche INRIA Lille – Nord Europe : Parc Scientifique de la Haute Borne - 40, avenue Halley - 59650 Villeneuve d'Ascq
Centre de recherche INRIA Nancy – Grand Est : LORIA, Technopôle de Nancy-Brabois - Campus scientifique
615, rue du Jardin Botanique - BP 101 - 54602 Villers-lès-Nancy Cedex
Centre de recherche INRIA Paris – Rocquencourt : Domaine de Voluceau - Rocquencourt - BP 105 - 78153 Le Chesnay Cedex
Centre de recherche INRIA Rennes – Bretagne Atlantique : IRISA, Campus universitaire de Beaulieu - 35042 Rennes Cedex
Centre de recherche INRIA Saclay – Île-de-France : Parc Orsay Université - ZAC des Vignes : 4, rue Jacques Monod - 91893 Orsay Cedex
Centre de recherche INRIA Sophia Antipolis – Méditerranée : 2004, route des Lucioles - BP 93 - 06902 Sophia Antipolis Cedex

Éditeur
INRIA - Domaine de Voluceau - Rocquencourt, BP 105 - 78153 Le Chesnay Cedex (France)
<http://www.inria.fr>
ISSN 0249-6399